

# Fluorofenidone attenuates renal fibrosis by inhibiting lysosomal cathepsin-mediated NLRP3 inflammasome activation

LINFENG ZHENG, WENJUAN MEI, JING ZHOU, XIN WEI, ZHIJUAN HUANG,  
XIAOZHEN LIN, LI ZHANG, WEI LIU, QIAN WU, JINHONG LI and YAN YAN

Department of Nephrology, The First Affiliated Hospital, Jiangxi Medical College,  
Nanchang University, Nanchang, Jiangxi 330006, P.R. China

Received July 14, 2023; Accepted January 30, 2024

DOI: 10.3892/etm.2024.12430

**Abstract.** Currently, no antifibrotic drug in clinical use can effectively treat renal fibrosis. Fluorofenidone (AKFPD), a novel pyridone agent, significantly reduces renal fibrosis by inhibiting the activation of the NOD-like receptor thermal protein domain associated protein 3 (NLRP3) inflammasome; however, the underlying mechanism of this inhibition is not fully understood. The present study aimed to reveal the molecular mechanism underlying the suppression of NLRP3 inflammasome activation by AKFPD. It investigated the effect of AKFPD on NLRP3 activation and lysosomal cathepsins in a unilateral ureteral obstruction (UUO) rat model, and hypoxia/reoxygenation (H/R)-treated HK-2 cells and murine peritoneal-derived macrophages (PDMs) stimulated with lipopolysaccharide (LPS) and ATP. The results confirmed that AKFPD suppressed renal interstitial fibrosis and inflammation by inhibiting NLRP3 inflammasome activation in UUO rat kidney tissues. In addition, AKFPD reduced the production of activated caspase-1 and maturation of IL-1 $\beta$  by suppressing NLRP3 inflammasome activation in H/R-treated HK-2 cells and murine PDMs stimulated with LPS and ATP. AKFPD also decreased the activities of cathepsins B, L and S both *in vivo* and *in vitro*. Notably, AKFPD downregulated cathepsin B expression and NLRP3 colocalization in the cytoplasm after lysosomal disruptions. Overall, the results suggested that AKFPD attenuates renal fibrosis by inhibiting lysosomal cathepsin-mediated activation of the NLRP3 inflammasome.

## Introduction

Renal interstitial fibrosis, a progressive pathological phenomenon, is a prominent feature of chronic kidney disease in humans and animal models (1,2). Renal interstitial fibrosis is also the final common pathway leading to end-stage kidney disease (3). Chronic renal inflammation promotes the progression of renal fibrosis by stimulating leukocyte infiltration into the kidneys and activating intrinsic renal cells to release profibrotic factors that drive renal fibrosis (4). Therefore, regulating inflammation is a key factor in treating renal fibrosis (5).

NOD-like receptor thermal protein domain associated protein 3 (NLRP3) forms a multi-protein immune complex called the NLRP3 inflammasome, which is composed of NLRP3, apoptosis-associated speck-like protein containing a caspase recruitment domain (ASC) and pro-caspase-1 (6). NLRP3 inflammasome assembly is triggered by multiple signaling pathways, including those related to lysosomal disruption, reactive oxygen species (ROS) and extracellular ATP (7). NLRP3 inflammasome assembly activates the cysteine protease caspase-1, which results in the secretion of mature, biologically active IL-1 $\beta$ , thereby playing a central role in inflammation (8). NLRP3 inflammasome activation can occur in both immune and resident cells of the glomerulus. Previous studies using diverse animal models of kidney disease have shown that the NLRP3 inflammasome exerts important effects on renal inflammation and fibrosis (9-11). Kim *et al* (12) have demonstrated, using the unilateral ureteral obstruction (UUO) model, that NLRP3-knockout mice exhibit reduced renal fibrosis and inflammation compared with wild-type mice. Lysosomal cathepsins are mainly located in lysosomes but can also function in the cell plasma or extracellular matrix. To date, 15 human lysosomal cathepsins have been reported, of which cathepsin B, D, S and L play an important role in renal physiopathology. Furthermore, NLRP3 inflammasome activation promotes renal inflammation, leading to glomerular damage and end-stage kidney disease in chronic kidney disease models (13-15). The expression of lysosomal cathepsins is significantly elevated in UUO mice, suggesting that pharmacological inhibition of cathepsins may lead to the alleviation of kidney fibrosis (14). In addition, small interfering (si)RNA knockdown of cathepsins B, L and S (CTSB, CTSL and CTSS, respectively) inhibits NLRP3 inflammasome activation by

---

*Correspondence to:* Professor Yan Yan, Department of Nephrology, The First Affiliated Hospital, Jiangxi Medical College, Nanchang University, 17 Yongwai Street, Nanchang, Jiangxi 330006, P.R. China  
E-mail: kiddoc@163.com

**Key words:** fluorofenidone, renal fibrosis, inflammation, lysosomal cathepsin, antifibrotic therapy

downregulating the production of pro-caspase-1 and pro-IL-1 $\beta$  in HK-2 cells (human tubular epithelial cell line) and mouse knockout models (16,17). Therefore, cathepsin-mediated NLRP3 inflammasome activation may be a therapeutic target in renal fibrosis.

Fluorofenidone [1-(3-fluorophenyl)-5-methyl-2-(H)-pyridone; AKFPD] is a novel low-molecular-weight pyridone agent. AKFPD exerts anti-inflammatory effects by reducing oxidative stress and apoptosis, ultimately suppressing fibrosis in the kidneys, liver and lungs (18-22). Fluorofenidone is associated with decreased inflammatory burden (23). By contrast, conditions that cause renal fibrosis, diabetic nephropathy for example, are associated with high burden of inflammation (24). A number of inflammatory markers, including C-reactive protein (25), serum uric acid (26) and systemic inflammatory index (27), are increased in diabetic nephropathy. Hence, studying the effects of Fluorofenidone in renal fibrosis makes sense. Our previous study demonstrated that AKFPD reduces IL-1 $\beta$  production by suppressing NLRP3 inflammasome activation in UUO rats, suggesting that AKFPD is a new anti-inflammatory agent (28). Furthermore, a recent study has reported that AKFPD attenuates renal fibrosis by inhibiting the mitochondrial ROS (mtROS)-NLRP3 pathway in a murine model of folic acid nephropathy (29). Nonetheless, the effect of AKFPD on the NLRP3 inflammasome in renal intrinsic cells remains unclear. In addition, the potential underlying mechanisms of the suppression of NLRP3 inflammasome activation by AKFPD in renal inflammation remain largely unknown. Therefore, the present study aimed to investigate the underlying mechanism of AKFPD in suppressing NLRP3 inflammasome activation in UUO rats. The study findings provided insights into understanding the anti-inflammatory and anti-fibrotic effects of AKFPD against renal fibrosis.

## Materials and methods

**Ethics approval.** The present study protocol was reviewed and approved by the Medical Research Ethics Committee of The First Affiliated Hospital, Jiangxi Medical College, Nanchang University (Nanchang, China; approval no. 2020-1-59).

**Animals and experimental protocol.** Male Sprague Dawley rats (8 weeks old; 180-220 g; n=30) were purchased from Silaike Laboratory Animal Co. Ltd. The rats were housed in a pathogen-free environment at 25 $\pm$ 2°C with 55 $\pm$ 2% humidity and under a 12-h light/dark cycle and provided a standard diet and tap water *ad libitum*. The rats were randomly divided into six groups: The 3- and 7-day sham-operated (sham group), 3- and 7-day UUO model (UUO group), and 3- and 7-day AKFPD treatment groups (AKFPD group), with five rats in each group. The UUO model was established by ligating the left ureter in the UUO and AKFPD groups, as previously described (30). Similar surgical procedures were performed in the sham group; however, the left ureter was only exposed and not ligated. AKFPD (lot no. 20190810) was obtained from the Haikou Pharmaceutical Factory Co., Ltd. The rats in the sham and UUO groups were gavaged daily with 0.5% sodium carboxymethyl cellulose (cat. no. 11926043; Shanghai Aladdin Biochemical Technology Co., Ltd.), whereas the rats in the AKFPD group received 500 mg/kg/day AKFPD dissolved

in 0.5% sodium carboxymethyl cellulose. AKFPD and the vehicle were administered starting day 1 after surgery until the day of euthanasia. The rats were administered 1% sodium pentobarbital (cat. no. 0123A001; MilliporeSigma) and sacrificed 3 and 7 days after surgery. Rats were anesthetized by intraperitoneal injection of sodium pentobarbital (60 mg/kg) for UUO operation. Rats were sacrificed by intraperitoneal injection of overdoses of sodium pentobarbital (150 mg/kg) for harvesting renal tissue. A portion of the left kidney was excised, and samples were fixed in 10% neutral-buffered formalin and 2.5% glutaraldehyde phosphate buffer (pH 7.4) for pathological examination. The remaining kidney tissue was preserved in liquid nitrogen for further experiments.

**Histopathology.** The kidney tissue samples were fixed with 4% paraformaldehyde for 24 h at 4°C. A section of the harvested left kidney was soaked in 70 and 80% alcohol for 30 min each, followed by soaking in 95% ethanol for 30 min (x2 times) and anhydrous ethanol for 30 min, and then soaked in xylene for 15 min. Finally, the sample was placed in the embedding box and soaked in wax at 60°C for 2 h. The paraffin-embedded kidney tissue was sliced into 4  $\mu$ m-thick sections and stained with hematoxylin-eosin (H&E) and Masson's trichrome. For H&E staining, a tissue section was incubated with hematoxylin for 10 min and eosin for 5 min, both at room temperature, and rinsed under running water. Masson trichrome staining was performed using the Trichrome Stain (Masson) Kit (cat. no. G1006; Wuhan Servicebio Technology Co., Ltd.) at room temperature, apart from Masson A staining, which was incubated for 30 min at 65°C. Tubulointerstitial injury was quantified based on the degree of renal interstitial fibrosis, tubular dilatation, atrophy, tubular epithelial injury, inflammatory cell infiltration and interstitial edema. Tubulointerstitial fibrosis was assessed in Masson's trichrome-stained sections. H&E staining sections were randomly selected from 5 renal interstitial fields, including upper left, lower left, middle, upper right and lower right, under an optical microscope at a x200 magnification. The renal interstitial injury score was assigned in a single blinded manner. The H&E score and tubulointerstitial fibrosis degree were determined as previously described (31). The samples were visualized using an Olympus light microscope (BX43; Olympus Corporation).

**Enzyme-linked immunosorbent assay (ELISA).** Levels of TNF- $\alpha$  and IL-1 $\beta$  in kidney homogenates were determined using specific ELISA kits (cat. nos. MM-0180R1, MM-0047R1; Elabscience Biotechnology, Inc.) according to the manufacturer's instructions.

**HK-2 cell culture and treatment.** HK-2 cell line was purchased from Beijing Beina Chuanglian Biotech Institute (cat. no. BNCC295660). The cells were cultured in a mixture of Dulbecco's modified Eagle medium and Ham's F-12 medium (Nanjing KeyGen Biotech Co., Ltd.) supplemented with 10% fetal bovine serum (FBS), 100 U/ml penicillin, and 100  $\mu$ g/ml streptomycin under a humidified atmosphere of 5% CO<sub>2</sub> and 95% O<sub>2</sub> at 37°C. The cells were seeded in six-well culture plates and cultured in a complete medium. The plates were randomly divided into three groups: Normal (N), hypoxia/reoxygenation (H/R) and AKFPD. The cells in the AKFPD and H/R groups

were cultured for 12 h at 37°C in a medium without nutrients (serum- and glucose-free) under hypoxic conditions (1% O<sub>2</sub>, 94% N<sub>2</sub> and 5% CO<sub>2</sub>) to induce hypoxic injury, and the cells were then transferred back to a regular culture medium with oxygen for 6 h at 37°C to facilitate reoxygenation. The normal group cells were incubated in a complete culture medium under regular incubator conditions (5% CO<sub>2</sub> and 95% air). The cells in the AKFPD group were pre-incubated at 37°C with 400 µg/ml AKFPD for 24 h.

**Isolation and culture of peritoneal-derived macrophages (PDMs).** PDMs were isolated from 50 male C57BL/6 mice (6-8 weeks old, 20-25 g), purchased from Shanghai SLAC Laboratory Animal Co., Ltd. The C57BL/6 mice were housed under controlled conditions at a temperature of 25±2°C with a 12-h light-dark cycle and 55±2% relative humidity, as previously described (32). Mice were and sacrificed by intraperitoneal injection of overdoses of sodium pentobarbital (150 mg/kg). PDMs were cultured in an RPMI 1640 medium supplemented with 10% FBS, 100 U/ml penicillin and 100 µg/ml streptomycin in a humidified atmosphere under 5% CO<sub>2</sub> and 95% O<sub>2</sub> at 37°C. Cells were randomly separated into three groups: Normal (N), LPS+ATP and AKFPD groups. PDMs in the LPS+ATP group were stimulated with 500 ng/ml lipopolysaccharide (LPS; cat. no. L8880; Beijing Solarbio Science & Technology Co., Ltd.) for 2.5 h, followed by exposure to 5 mM ATP (cat. no. 10519979001; Roche Diagnostics) for 0.5 h at 37°C. PDMs in the AKFPD group were pre-incubated with 400 µg/ml AKFPD for 24 h at 37°C and subsequently exposed to LPS plus ATP.

**Immunofluorescence.** The kidney tissue sections were fixed in 4% paraformaldehyde for 24 h at 4°C. The kidney tissue samples were soaked in 70, 80 and 95% ethanol and anhydrous ethanol, followed by embedding in paraffin and slicing into 4 µm-thick sections, followed by permeabilization with 0.5% Triton X-100 in PBS for 20 min at 37°C. After blocking with 5% bovine serum albumin (cat. no. A8020; Solarbio) for 30 min at 37°C, the sections were incubated with primary antibodies against myeloperoxidase (MPO; 1:100 dilution; cat. no. 22225-1-AP; Proteintech Group, Inc.) overnight at 4°C. The slides were then incubated with goat anti-rabbit secondary antibody (cat. no. AS007; ABclonal Biotech Co., Ltd.) at 37°C for 45 min. The cell nuclei were counterstained with DAPI (cat. no. KGA215-50; Nanjing KeyGen Biotech Co., Ltd.) for 3 min at 37°C.

To detect colocalization using immunofluorescence, kidney tissues or cells were separately incubated with anti-NLRP3 (1:100 dilution; cat. no. AG-20B-0006; AdipoGen Life Sciences), anti-cathepsin B (1:150; cat. no. 12216-1-AP; Proteintech Group, Inc.) and anti-ASC (1:200; cat. no. bs-6741R; Bioss Antibodies) antibodies in a humidified chamber overnight at 4°C, followed by incubation with secondary antibodies Cy3 goat anti-rabbit IgG (1:200; cat. no. AS007; ABclonal) and Goat anti rabbit IgG/488 (1:100; cat. no. ZF-0511; ZSGB-BIO) for 45 min at 37°C. The cell nuclei were stained with DAPI. The immunostained samples were visualized under a CKX53 confocal microscope (Olympus Corporation). The quantitative changes were measured using Image-Pro Plus 6.0 (Media Cybernetics).

For lysosome detection, HK-2 cells and PDMs were incubated with LysoTracker Red stain (cat. no. C1046; Beyotime Institute of Biotechnology) for 1 h at 37°C. After washing with PBS three times, the cells were fixed with 4% paraformaldehyde for 10 min and stained with DAPI for 20 min at 37°C. The cells were examined using a confocal microscope (CKX53; Olympus Corp.) and representative images were captured. The *in vitro* experiments were performed in triplicate.

**Cathepsin activity assay.** After processing the cells and kidney tissues, specific activity assay kits (cat. nos. ab65306, ab65307 and ab65300; Abcam) were used to detect the activities of CTSL, CTSS and CTSB, according to the manufacturer's instructions. Fluorescence was quantified using an automatic microplate reader (Beijing Liuyi Biotechnology Co. Ltd.) at excitation/emission wavelengths of 400/505 nm.

**Western blot analysis.** The protein lysates from cultured cells and kidney tissues were prepared as previously described (33), tissues and cells were lysed by RIPA lysate buffer (cat. no. C1053; Applygen Technologies, Inc.) and total protein was extracted. The protein content was determined using a BCA protein assay kit (cat. no. E-BC-K318-M; Elabscience Biotechnology, Inc.). Subsequently, 20-40 µg of total protein was loaded per lane for SDS-PAGE. Proteins were separated by 8-15% SDS-PAGE under reducing conditions and transferred onto PVDF membranes (cat. no. IVPH00010; MilliporeSigma). The membranes were blocked in 3% non-fat dry milk (cat. no. P1622; Beijing Pulilai Gene Technology Co., Ltd.) in Tris-buffered saline with 0.1% Tween 20 detergent (TBS-T) at 37°C for 1 h, followed by incubation with primary antibodies overnight at 4°C. The membranes were then incubated with secondary antibodies at 37°C for 2 h. ECL western blotting detection reagent (Thermo Fisher Scientific, Inc.) was used to visualize the protein bands, which were quantified using the Tanon-5200 automatic chemiluminescence image analysis system (Tanon Science and Technology Co., Ltd.). The intensity is expressed as the relative protein expression, which was normalized to the expression of β-actin. Image J software V1.8.0 (National Institutes of Health) was adopted for the analysis of the grayscale of the protein bands.

The following primary antibodies were used: Anti-fibronectin (FN; 1:1,000 dilution; cat. no. ab268023; Abcam), anti-α-smooth muscle actin (α-SMA; 1:1,000; cat. no. ab124964; Abcam), anti-NLRP3 (1:1,000; cat. no. AG-20B-0006; AdipoGen Life Sciences), anti-ASC (1:1,000; cat. no. bs-6741R; Bioss Antibodies), anti-CTSB (1:500; cat. no. 12216-1-AP; Proteintech Group, Inc.), anti-caspase-1 (1:1,000; cat. no. ab179515; Abcam), anti-IL-1β (1:500; cat. no. sc-7884; Santa Cruz Biotechnology, Inc.) and anti-β-actin (1:2,000; cat. no. TA-09; OriGene Technologies, Inc.). The secondary horseradish peroxidase-conjugated antibodies used were anti-rabbit IgG (1:2,000; cat. no. ZB-2301; ZSGB-BIO) and anti-mouse IgG (1:2,000; cat. no. ZB-2305; ZSGB-BIO).

**Statistical analysis.** All experiments were performed at least three times, and data are expressed as mean ± standard deviation for each group, with the exception of the H&E

scores, which were expressed using median and interquartile ranges (IQR). Statistical analysis was performed using IBM SPSS Statistics for Windows, version 19 (IBM Corp.). The Shapiro-Wilk normality test was used to test normality. Comparisons between groups were conducted using a one-way analysis of variance followed by Bonferroni analysis. For analysis of H&E scores, the non-parametric Kruskal-Wallis H-test was applied.  $P < 0.05$  was considered to indicate a statistically significant difference.

## Results

*AKFPD ameliorates renal fibrosis in UUO rats.* As indicated in Fig. 1, H&E staining revealed that the kidney tissues of UUO rats had the typical features of tubulointerstitial injury, including tubular damage, inflammatory cell infiltration and interstitial fibrosis ( $P < 0.01$ ; Fig. 1A and C). These changes were attenuated by treatment with AKFPD on days 3 and 7 post-surgery ( $P < 0.01$ ; Fig. 1A and C). Renal interstitial fibrosis evaluated using Masson's trichrome staining indicated that the tubulointerstitial fibrosis index of the UUO group was higher than that of the sham group ( $P < 0.01$ ; Fig. 1B and D). However, the degree of renal interstitial fibrosis was reduced by treatment with AKFPD on days 3 and 7 post-surgery ( $P < 0.01$ ; Fig. 1B and D).

Western blotting results indicated that the expression of key fibrotic proteins (FN and  $\alpha$ -SMA) was markedly increased in the UUO group on days 3 and 7 post-surgery compared with that in the sham group ( $P < 0.01$ ; Fig. 1E and F). Furthermore, the expression of fibrotic proteins FN and  $\alpha$ -SMA was decreased by treatment with AKFPD ( $P < 0.01$ ; Fig. 1E and F). The results showed that AKFPD alleviated renal fibrosis in the UUO model.

*AKFPD suppresses renal inflammation in UUO rats.* Chronic renal inflammation promotes the occurrence and progression of renal fibrosis. Renal inflammation is mainly associated with inflammatory cytokines, such as IL-1 $\beta$  and TNF- $\alpha$ , and infiltration of inflammatory cells, including neutrophils and macrophages (34,35). To explore the effect of AKFPD on renal inflammation, the abundance of MPO-positive cells in the kidney tissue was determined using immunofluorescence (Fig. 2) because MPO is expressed in activated macrophages, monocytes and neutrophils (36). MPO-positive cells were mainly distributed around the renal tubules. As shown in Fig. 2A and C, the number of infiltrating MPO-positive cells was significantly increased in the UUO group on days 3 and 7 post-surgery compared with that in the sham group. However, the number of infiltrating MPO-positive cells decreased after treatment with AKFPD ( $P < 0.05$ ).

Furthermore, the ELISA results revealed that the expression of the inflammatory cytokines IL-1 $\beta$  and TNF- $\alpha$  was significantly elevated in the UUO group on days 3 and 7 post-surgery compared with that in the sham group. However, these elevated IL-1 $\beta$  and TNF- $\alpha$  levels decreased after treatment with AKFPD treatment ( $P < 0.05$ ; Fig. 2D and E). In conclusion, these results suggested that AKFPD reduces the expression of inflammatory factors and the infiltration of inflammatory cells in the UUO model.

*AKFPD suppresses NLRP3 inflammasome activation in UUO rats.* NLRP3 inflammasome activation accelerates the progression of renal fibrosis in UUO models (37,38). In the present study, western blotting demonstrated that the protein levels of NLRP3, ASC, pro-caspase-1, caspase-1, pro-IL-1 $\beta$  and IL-1 $\beta$  were elevated in the UUO group on days 3 and 7 post-surgery compared with those in the sham group (Fig. 3). The protein levels of activated caspase-1 and IL-1 $\beta$  were significantly reduced by treatment with AKFPD ( $P < 0.01$ ; Fig. 3). There was a slight increase in the NLRP3, ASC, pro-caspase-1 and pro-IL-1 $\beta$  protein expression in the AKFPD group, but no statistically significant difference with the UUO group ( $P > 0.05$ ; Fig. 3). These results suggested that AKFPD effectively down-regulated activated caspase-1 expression and IL-1 $\beta$  secretion by suppressing NLRP3 inflammasome activation.

*AKFPD inhibits NLRP3 inflammasome activation in vitro.* Macrophage-mediated inflammatory responses play an integral role in the progression of kidney fibrosis (39). To investigate the mechanism by which AKFPD suppresses NLRP3 inflammasome activation, LPS and ATP were used to stimulate mouse PDMs to activate the NLRP3 inflammasome *in vitro* (Fig. 4). The western blotting results indicated that the protein levels of NLRP3, ASC, pro-caspase-1, pro-IL-1 $\beta$ , caspase-1 and IL-1 $\beta$  were substantially increased in stimulated PDMs compared with those in normal cells; however, these elevated levels were significantly decreased by treatment with AKFPD ( $P < 0.05$ ; Fig. 4A and B). Colocalization of NLRP3 with ASC in the cytoplasm was increased in stimulated PDMs (reflected by increased yellow immunofluorescent staining) compared with that in normal cells ( $P < 0.01$ ; Fig. 4E and G), whereas NLRP3-ASC binding decreased by treatment with AKFPD ( $P < 0.05$ ; Fig. 4E and G). In addition to macrophages, NLRP3 inflammasome activation was investigated in HK-2 cells (40,41). The protein levels of NLRP3, ASC, pro-caspase-1, caspase-1, pro-IL-1 $\beta$  and IL-1 $\beta$  were increased in the H/R group compared with those in the normal group ( $P < 0.05$ ; Fig. 4C and D) and these increases were reversed by treatment with AKFPD ( $P < 0.05$ ; Fig. 4C and D). As shown in Fig. 4F, confocal microscopy demonstrated that the colocalization of NLRP3 with ASC was remarkably increased in H/R-treated HK-2 cells (reflected by increased yellow staining) compared with that in the normal group ( $P < 0.01$ ; Fig. 4F and H) and this increase was rescued by treatment with AKFPD ( $P < 0.01$ ; Fig. 4F and H). Overall, *in vitro* results indicated that AKFPD reduced the production of inflammatory factors by inhibiting NLRP3 inflammasome.

*AKFPD attenuates lysosomal cathepsin activities in vitro.* The NLRP3 inflammasome can be activated by danger signals, including potassium efflux, lysosomal cathepsin leakage and mtROS formation. Previous studies using cathepsin knockout or knockdown models have revealed that multiple cathepsins are involved in NLRP3 inflammasome activation (16,42). Therefore, it was hypothesized that AKFPD suppressed NLRP3 inflammasome activation by downregulating lysosomal cathepsin activity. As indicated in Fig. 5, the cathepsin activity assay indicated that the activities of CTSB, CTSS and CTSL were markedly elevated in LPS/ATP-stimulated PDMs and H/R-treated HK-2 cells compared with those in normal cells, whereas they were significantly decreased after treatment with AKFPD ( $P < 0.05$ ;

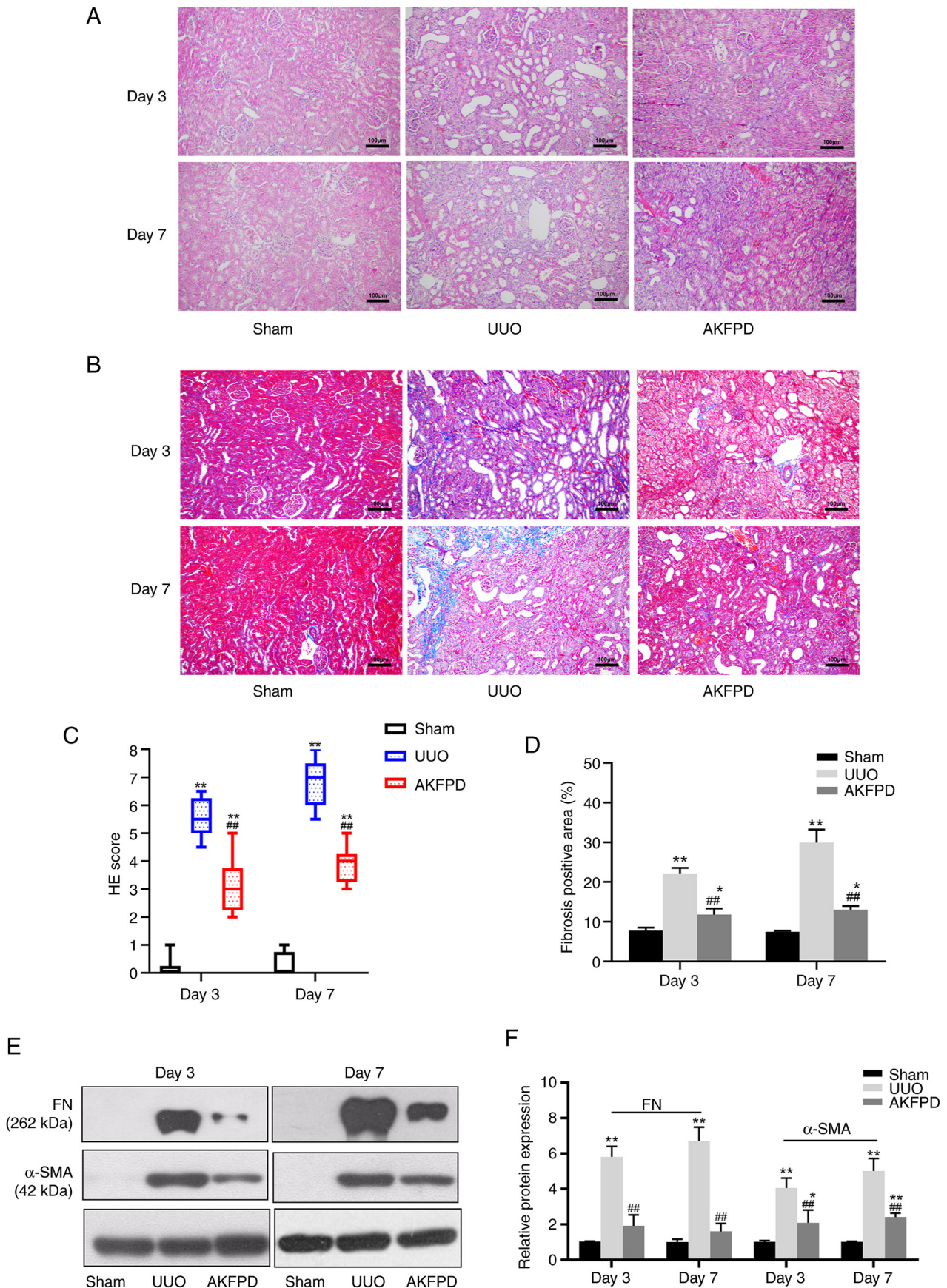


Figure 1. AKFPD ameliorates renal fibrosis in the kidney tissue of UUO rats on days 3 and 7 after surgery. (A) H&E staining of representative rat kidney tissue sections (scale bar, 100  $\mu$ m). (B) Masson's trichrome staining of representative rat kidney tissue sections. (scale bar, 100  $\mu$ m). (C) H&E score for kidney damage. (D) The tubulointerstitial fibrosis index is indicated. (E) Representative western blots of FN and  $\alpha$ -SMA in the rat kidney tissue. (F) Quantitative analysis of FN and  $\alpha$ -SMA protein expression in the rat kidney tissue. H&E scores are expressed using median and interquartile range, with the rest of the data are expressed as mean  $\pm$  standard deviation (n=5 per group). \* $P$ <0.05 vs. sham group, \*\* $P$ <0.01 vs. sham group, ## $P$ <0.01 vs. UUO group. AKFPD, fluorofenidone; UUO, unilateral ureteral obstruction; H&E, hematoxylin-eosin; FN, fibronectin;  $\alpha$ -SMA,  $\alpha$ -smooth muscle actin.

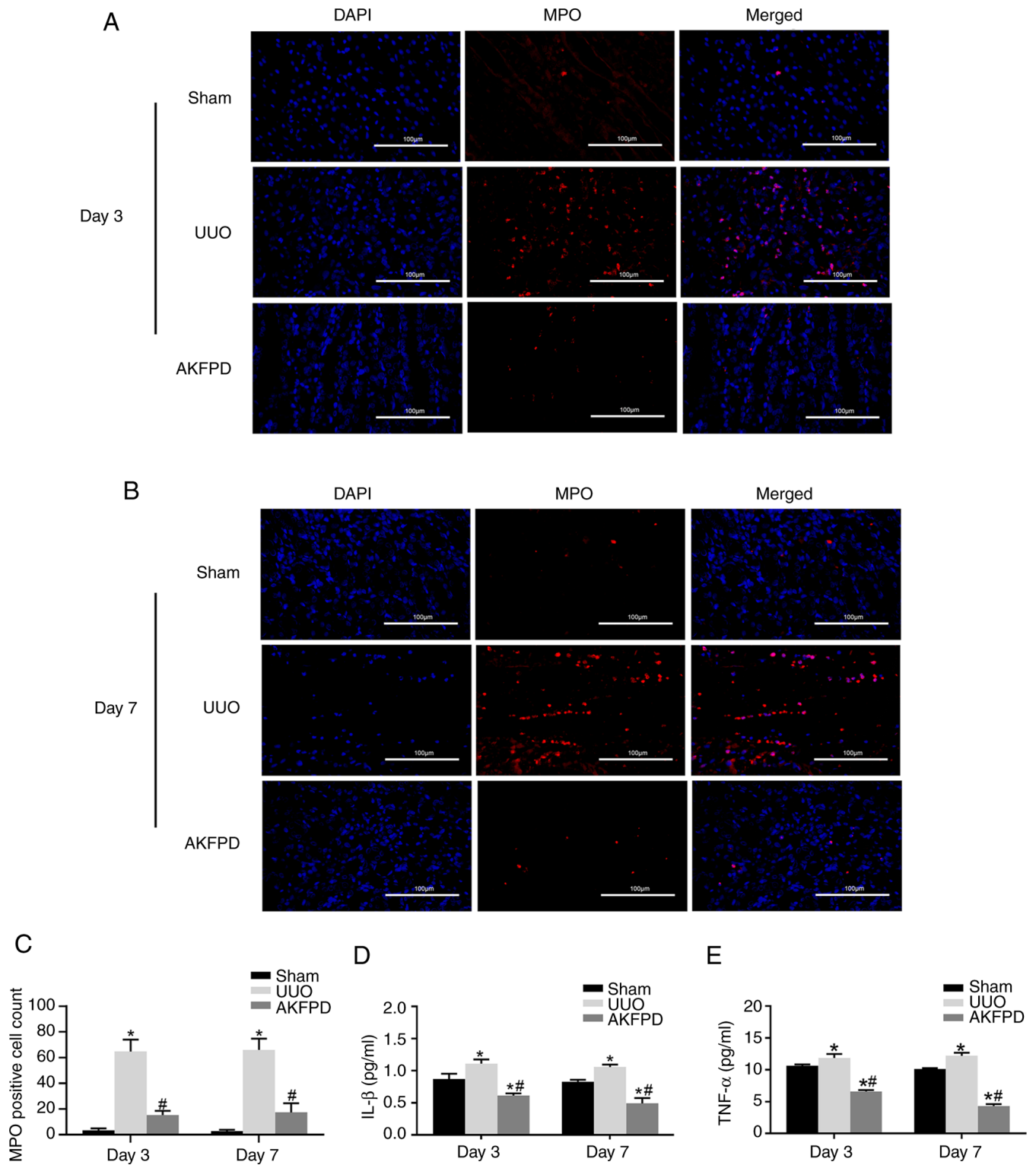


Figure 2. AKFPD suppresses renal inflammation in UUO rats. (A and B) Immunofluorescence of MPO-positive cells in rat kidney tissues (magnification,  $\times 200$ ; scale bars,  $100 \mu\text{m}$ ). (C) Quantification of MPO-positive cells in five fields. (D) ELISA of IL-1 $\beta$  expression in the rat kidney tissues. (E) ELISA of TNF- $\alpha$  expression in the rat kidney tissue. Data are presented as mean  $\pm$  standard deviation ( $n=5$  per group). \* $P<0.05$  vs. sham group, # $P<0.05$  vs. UUO group. AKFPD, fluorfenidone; UUO, unilateral ureteral obstruction; MPO, myeloperoxidase.

Fig. 5A and C). In addition, LysoTracker Red dye was used to label acidic lysosomes, revealing that LPS/ATP-stimulated PDMs and H/R-treated HK-2 cells exhibited significantly increased numbers of lysosomes or induced lysosome aggregation compared with those in normal cells ( $P<0.01$ ; Fig. 5B and D-F), and this effect was inhibited after treatment with AKFPD ( $P<0.01$ ; Fig. 5B and D-F).

The results showed that AKFPD protected lysosomal damage and downregulated lysosomal cathepsins activity *in vitro*.

AKFPD suppresses NLRP3 inflammasome activation by decreasing cathepsin B expression *in vitro*. CTSB is required for IL-1 $\beta$  production and is induced by a diverse set of

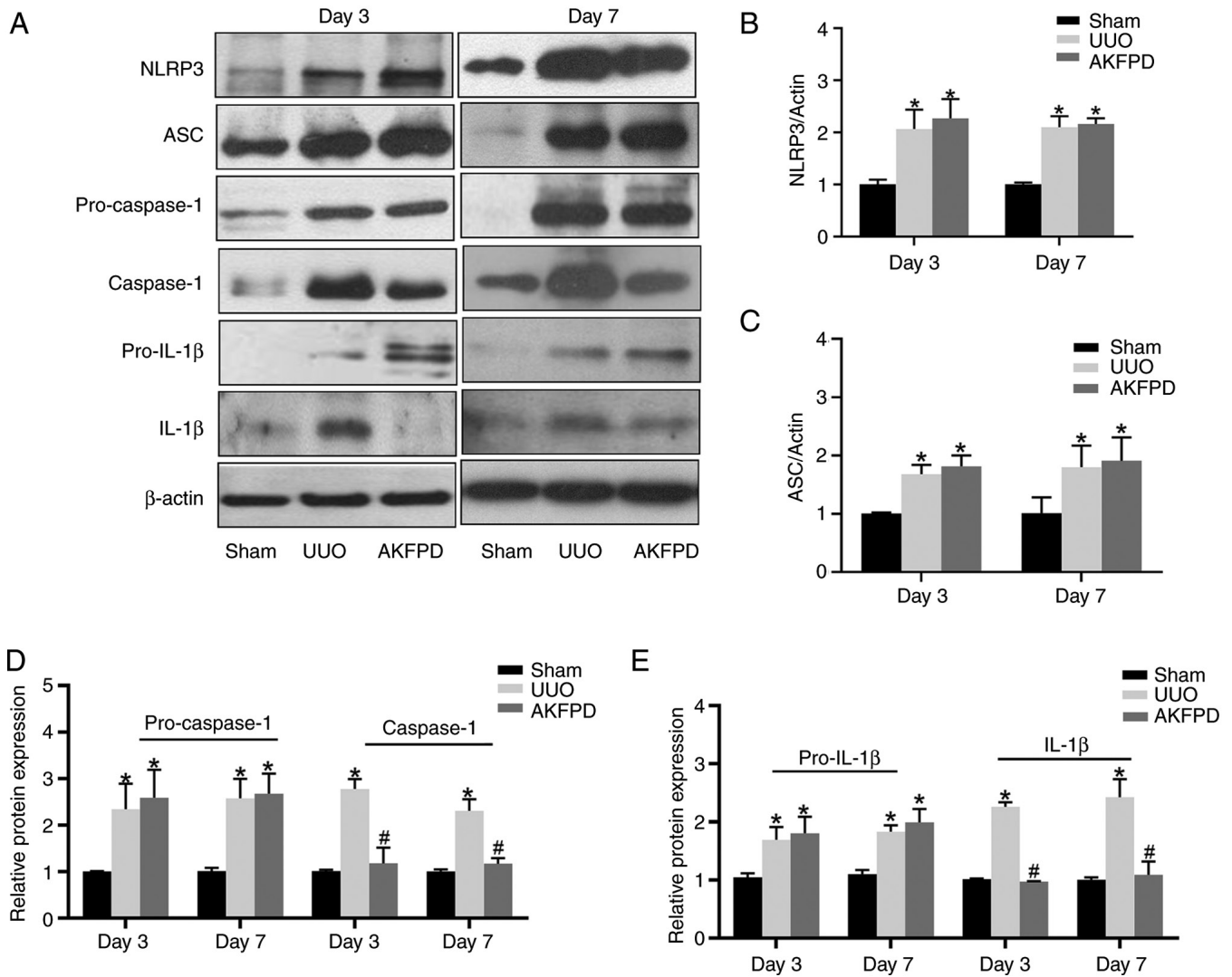


Figure 3. AKFPD inhibits NLRP3 inflammasome activation in UUO rats. (A) Representative western blot of NLRP3, ASC, pro-caspase-1, pro-IL-1 $\beta$ , caspase-1 and IL-1 $\beta$  expression in the rat kidney tissues on days 3 and 7 post-surgery. (B-E) Quantitative analysis of (B) NLRP3, pro-caspase-1, (C) ASC, (D) pro-caspase-1 and caspase-1, and (E) pro-IL-1 $\beta$  and IL-1 $\beta$  protein expression in rat kidney tissues. Data are presented as mean  $\pm$  standard deviation (n=5 per group). \*P<0.05 vs. sham group, #P<0.05 vs. UUO group. AKFPD, fluorofenidone; NLRP3, NOD-like receptor thermal protein domain associated protein 3; UUO, unilateral ureteral obstruction; ASC, apoptosis-associated speck-like protein containing a caspase recruitment domain.

NLRP3 inflammasome activators (43). Lysosomal cathepsins, especially CTSB, activate the NLRP3 inflammasome via direct interactions (44). As presented in Fig. 6, in the present study, western blotting indicated that the CTSB protein level was significantly increased in LPS/ATP-stimulated PDMs compared with that in normal cells (P<0.05; Fig. 6A), and the same results were observed in H/R-treated HK-2 cells (P<0.05; Fig. 6D). However, treatment with AKFPD decreased the elevated CTSB protein level *in vitro* (P<0.05; Fig. 6A and D). The expression and colocalization of CTSB with NLRP3 were evaluated *in vitro* using immunofluorescence for further validation. The immunostaining results indicated a low association between CTSB and NLRP3 in normal cells. By contrast, LPS/ATP-stimulated PDMs and H/R-treated HK-2 cells exhibited increased colocalization of CTSB with NLRP3 compared with that in normal cells (P<0.01; Fig. 6B, C, E and F). These results suggested that CTSB was released from lysosomes and colocalized with NLRP3 in the cytoplasm under inflammatory conditions

induced by LPS/ATP stimulation or H/R treatment. As predicted, these changes were abrogated by treatment with AKFPD (P<0.05; Fig. 6B, C, E and F). These findings support the hypothesis that AKFPD inhibited NLRP3 inflammasome activation by reducing the expression of CTSB protein *in vitro*.

**AKFPD inhibits NLRP3 inflammasome activation via the lysosome pathway in UUO rats.** To further confirm the mechanism underlying the aforementioned results, AKFPD suppression of cathepsin activity was investigated in UUO rats (Fig. 7). The activities of CTSB, CTSS and CTSL were significantly increased in the UUO group compared with those in the sham group on days 3 and 7 post-surgery (P<0.05; Fig. 7A) and were significantly decreased after treatment with AKFPD (P<0.05; Fig. 7A). Western blotting indicated that the CTSB protein expression level was elevated on days 3 and 7 post-surgery in the UUO group compared with that in the sham group. However, treatment with AKFPD reduced

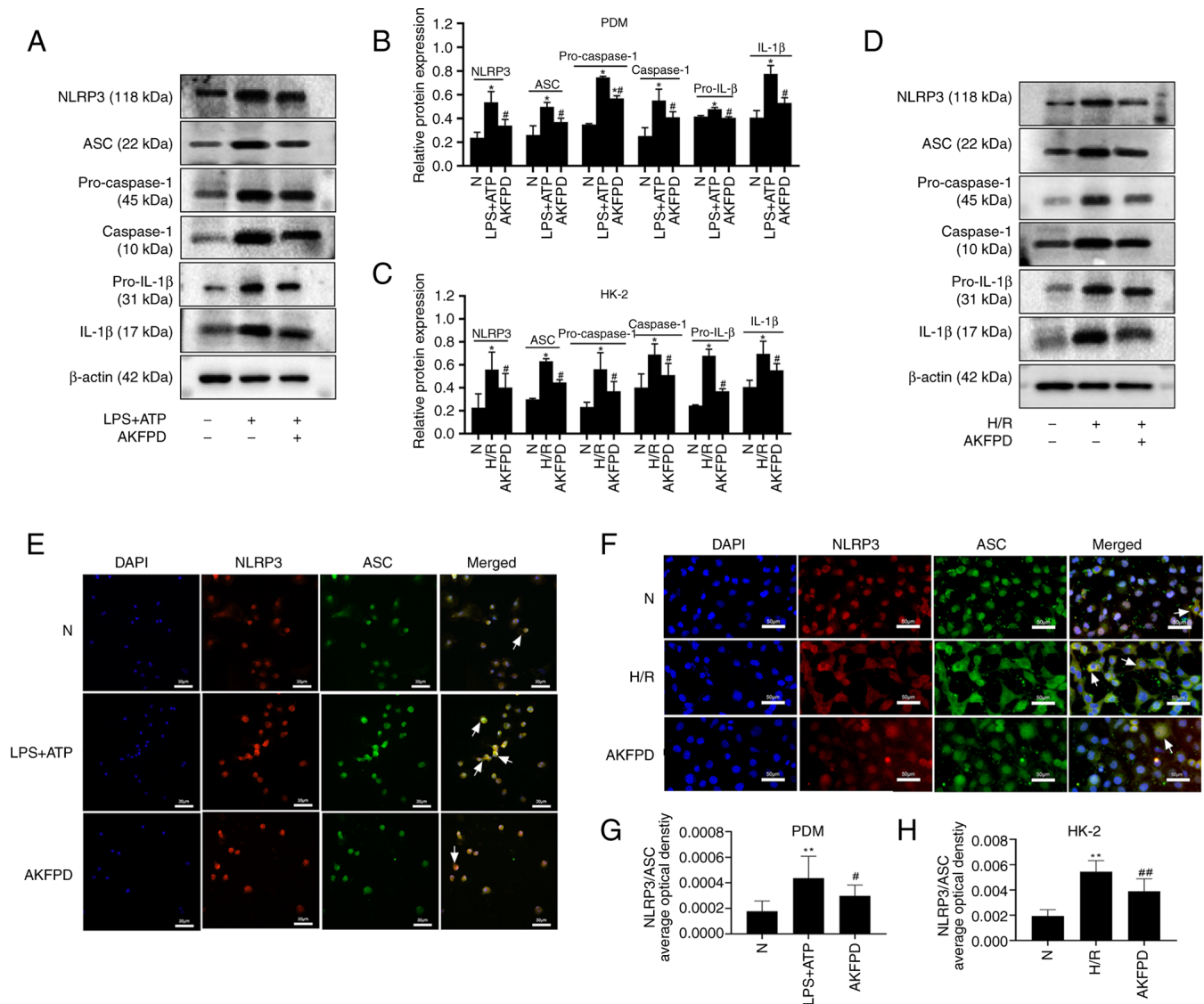


Figure 4. AKFPD inhibits NLRP3 inflammasome activation *in vitro*. (A) Representative western blot and (B) quantitative analysis of NLRP3, pro-IL-1 $\beta$ , caspase-1 and IL-1 $\beta$  expression in LPS/ATP-stimulated PDMs. (C) Representative western blot and (D) quantitative analysis of NLRP3, pro-IL-1 $\beta$ , caspase-1 and IL-1 $\beta$  expression in H/R-treated HK-2 cells. (E) Colocalization of NLRP3 and ASC in PDMs visualized using immunofluorescent staining. The white arrows indicate overlap (yellow). (magnification,  $\times 400$ ; scale bar,  $30 \mu\text{m}$ ). (F) Colocalization of NLRP3 and ASC in HK-2 cells visualized using immunofluorescent staining. The white arrows indicate overlap (yellow) (magnification,  $\times 400$ ; scale bar,  $50 \mu\text{m}$ ). (G) Quantification of the immunofluorescent co-localization of NLRP3 and ASC in PDMs. The quantitative changes were measured using Image-Pro Plus 6.0.  $^{\#}P<0.05$ .  $^{**}P<0.01$  vs. N group;  $^{\#}P<0.05$  vs. H/R group or vs. LPS+ATP group,  $^{##}P<0.01$  vs. H/R group. AKFPD, fluorfenidone; NLRP3, NOD-like receptor thermal protein domain associated protein 3; PDMs, peritoneal-derived macrophages; N, normal; H/R, hypoxia/reoxygenation; ASC, apoptosis-associated speck-like protein containing a caspase recruitment domain.

this increased CTSB expression level ( $P<0.05$ ; Fig. 7C and E). Subsequently, the immunofluorescence results indicated that the colocalization of CTSB with NLRP3 sharply increased in the UUO group on days 3 and 7 post-surgery compared with that in the sham group. However, it was significantly decreased after treatment with AKFPD (Fig. 7B and D). Taken together, the results suggest that AKFPD suppressed NLRP3 inflammasome activation via the lysosome pathway *in vivo*.

## Discussion

The final characteristic feature of end-stage kidney disease is renal fibrosis (45), for which there is no effective

clinical treatment. Chronic renal inflammation is an important contributor to chronic kidney disease. Renal inflammation is caused by macrophage accumulation and inflammatory cell infiltration in kidney tissues (35). Consistent with the findings of previous studies (46,47), the results of the present study indicated that AKFPD suppressed extracellular matrix deposition, decreased interstitial infiltration of inflammatory cells and downregulated inflammatory cytokine production in the kidney tissues of UUO rats. Furthermore, the results suggested that AKFPD attenuated renal fibrosis by suppressing leached lysosomal cathepsins, thereby further inhibiting the activation of the downstream cathepsin-NLRP3 inflammasome pathway in UUO rats. These findings provided new insights into a

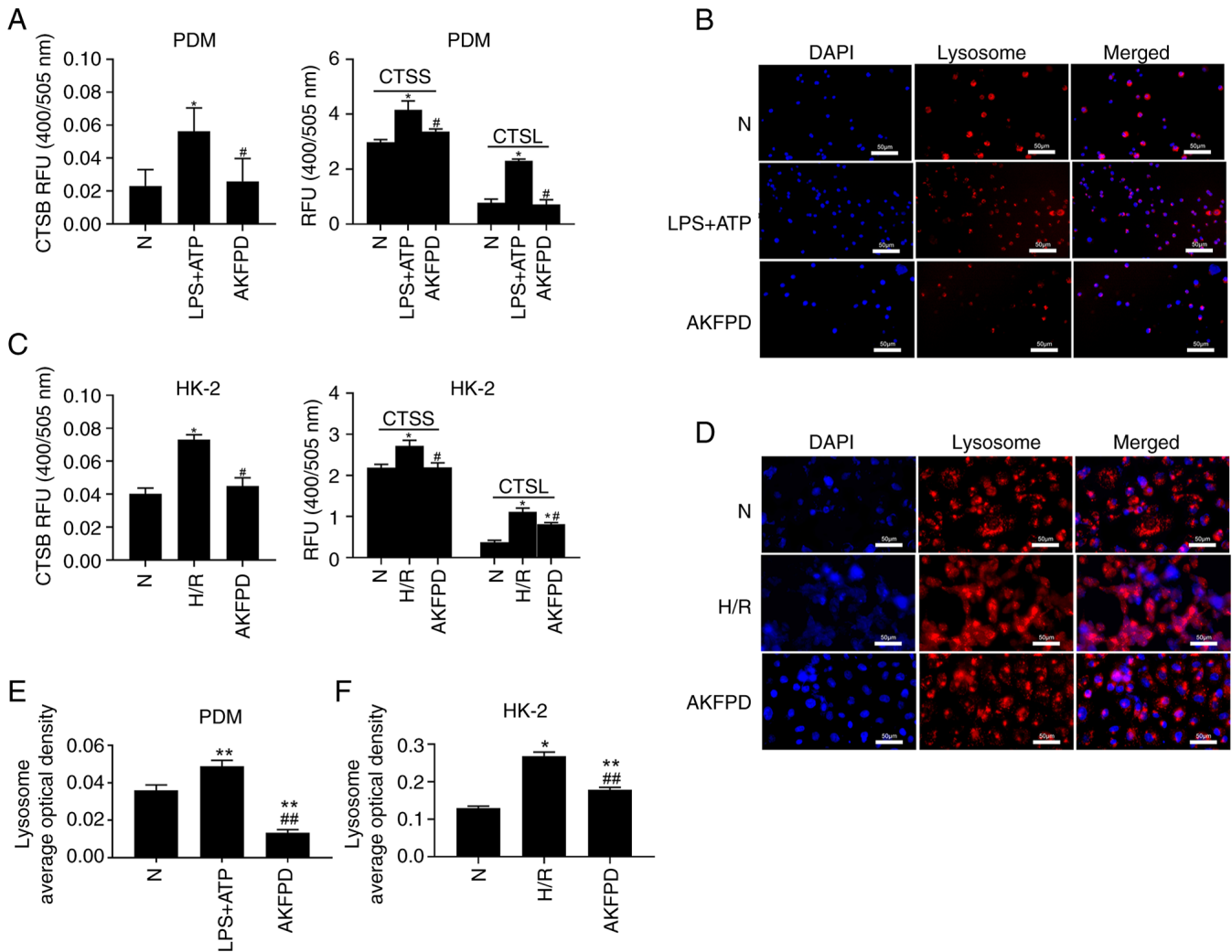


Figure 5. AKFPD downregulates cathepsin activity *in vitro*. (A) Effects of AKFPD on cathepsin (CTSB, CTSS and CTSL) activities in PDMs. (B) Effects of AKFPD on the accumulation of lysosomes visualized using LysoTracker Red dye in PDMs (magnification, x400; scale bar, 50  $\mu$ m). (C) Effects of AKFPD on cathepsin (CTSB, CTSS and CTSL) activities in HK-2 cells. (D) Effects of AKFPD on the accumulation of lysosomes visualized using LysoTracker Red dye in HK-2 cells (magnification, x400; scale bar, 50  $\mu$ m). (E) Quantitative analysis of the effect of AKFPD on lysosomes accumulation visualized in PDMs using LysoTracker red dye. (F) Quantitative analysis of the effect of AKFPD on lysosome accumulation visualized in HK-2 cells using LysoTracker red dye. Data are presented as mean  $\pm$  standard deviation (n=3 per group). \*P<0.05, \*\*P<0.01 vs. N group; #P<0.05 ##P<0.01 vs. H/R group or vs. LPS + ATP group. AKFPD, fluorofenidone; CTSB, cathepsin B; CTSS, cathepsin S; CTSL cathepsin L; N, normal; PDMs, peritoneal-derived macrophages; H/R, hypoxia/reoxygenation.

previously unknown molecular mechanism underlying the protective effects of AKFPD against renal fibrosis.

Emerging evidence indicates that the NLRP3 inflammasome, which comprises NLRP3, ASC and pro-caspase-1, promotes the development of renal fibrosis (48-50). The NLRP3 inflammasome acts as an important danger-recognition platform and can be activated by pathogen-associated molecular patterns and damage-associated molecular patterns (51). These two steps of initiation and activation are necessary for NLRP3 inflammasome activation. The initiation step (signal 1) is related to the NF- $\kappa$ B pathway and pro-IL-1 $\beta$  production whereas the activation step (signal 2) contributes to the oligomerization of the NLRP3 inflammasome and caspase-1-mediated secretion of IL-1 $\beta$  (52). The results of the present study demonstrated that the protein expression of NLRP3 inflammasome components was elevated and activated under renal fibrosis conditions both *in vivo* and *in vitro*. Furthermore, treatment with AKFPD significantly reduced

the expression of activated caspase-1 and secretion of IL-1 $\beta$  *in vivo*, indicating that NLRP3 inflammasome activation was significantly inhibited. However, AKFPD did not affect the protein levels of the NLRP3 inflammasome components NLRP3, ASC and pro-caspase-1. These results suggested that the inhibition of NLRP3 inflammasome activation underlies the anti-inflammatory effects of AKFPD in UUO rats. Notably, treatment with AKFPD significantly reduced the expression of NLRP3, ASC and pro-caspase-1 *in vitro*, suggesting it may affect the NF- $\kappa$ B pathway of the initiation signal (signal 1) *in vitro*. Additionally, AKFPD treatment also suppressed NLRP3 inflammasome activation in activated PDMs and H/R-treated HK-2 cells. Overall, the results suggest a common mechanism *in vivo* and *in vitro* by which AKFPD specifically suppresses NLRP3 inflammasome activation via the activation step (signal 2).

Lysosomal cysteine cathepsins are a family of enzymes that require an acidic, reducing environment for their

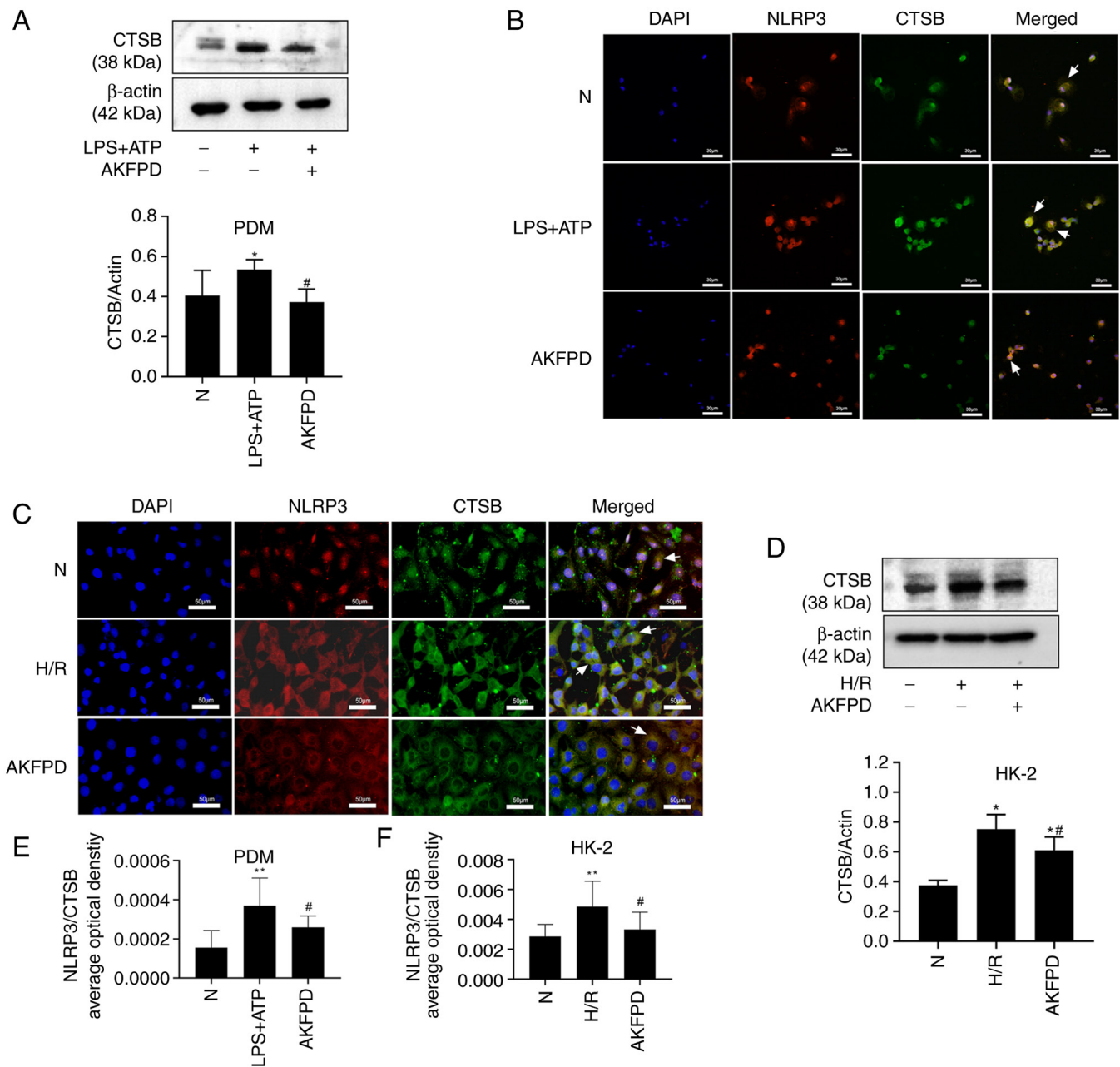


Figure 6. AKFPD inhibits NLRP3 inflammasome activation by CTSB expression *in vitro*. (A) Representative western blot and quantitative data of CTSB in LPS + ATP-stimulated PDMs. (B) Effects of AKFPD on the colocalization of NLRP3 and CTSB in activated PDMs visualized using immunofluorescent staining. White arrows indicate overlap (yellow) (magnification, x400; scale bar, 30  $\mu$ m). (C) Effects of AKFPD on the colocalization of CTSB and NLRP3 in H/R-treated HK-2 cells visualized using immunofluorescent staining. White arrows represent overlap (yellow) (magnification, x400; scale bar, 50  $\mu$ m). (D) Representative western blot and quantitative data of CTSB in H/R-treated HK-2 cells. (E) Quantitative analysis of the effect of AKFPD on NLRP3 and CTSB co-localization in activated PDM visualized using immunofluorescent staining. The quantitative changes were measured using Image-Pro Plus 6.0. (F) Quantitative analysis of the effect of AKFPD on the co-localization of CTSB and NLRP3 in H/R-treated HK-2 cells observed using immunofluorescent staining. The quantitative changes were measured using Image-Pro Plus 6.0. Data are presented as mean  $\pm$  standard deviation (n=3 per group). \* $P$ <0.05, \*\* $P$ <0.01 vs. N group; # $P$ <0.05 vs. H/R group or vs. LPS + ATP group. AKFPD, flufenidone; NLRP3, NOD-like receptor thermal protein domain associated protein 3; CTSB, cathepsin B; PDMs, peritoneal-derived macrophages; N, normal; H/R, hypoxia/reoxygenation.

activation. Previous studies have reported that multiple cathepsins exert a positive effect on NLRP3 inflammasome activation (17,53). siRNA knockdown of *CTSB*, *CTSL* and *CTSS* decreases the levels of caspase-1 and IL-1 $\beta$  in active PDMs and H/R-treated HK-2 cells, suggesting that NLRP3 inflammasome activation was inhibited (42). Another study demonstrated that lysosomal cathepsin expression is significantly elevated in UUO mice, suggesting that pharmacological blocking of cathepsin activity may help treat kidney

fibrosis (14). In the present study, the activities of lysosomal CTSB, CTSS and CTSL were increased in stimulated cells in which the NLRP3 inflammasome was activated but were notably decreased by treatment with AKFPD. The effect of AKFPD on the cathepsin-NLRP3 activation pathway was further confirmed in UUO rats, in which lysosomal disruption resulted in the release of cathepsins into the cytoplasm of kidney tissues; the cathepsins were then involved in NLRP3 inflammasome activation. Consistent with the

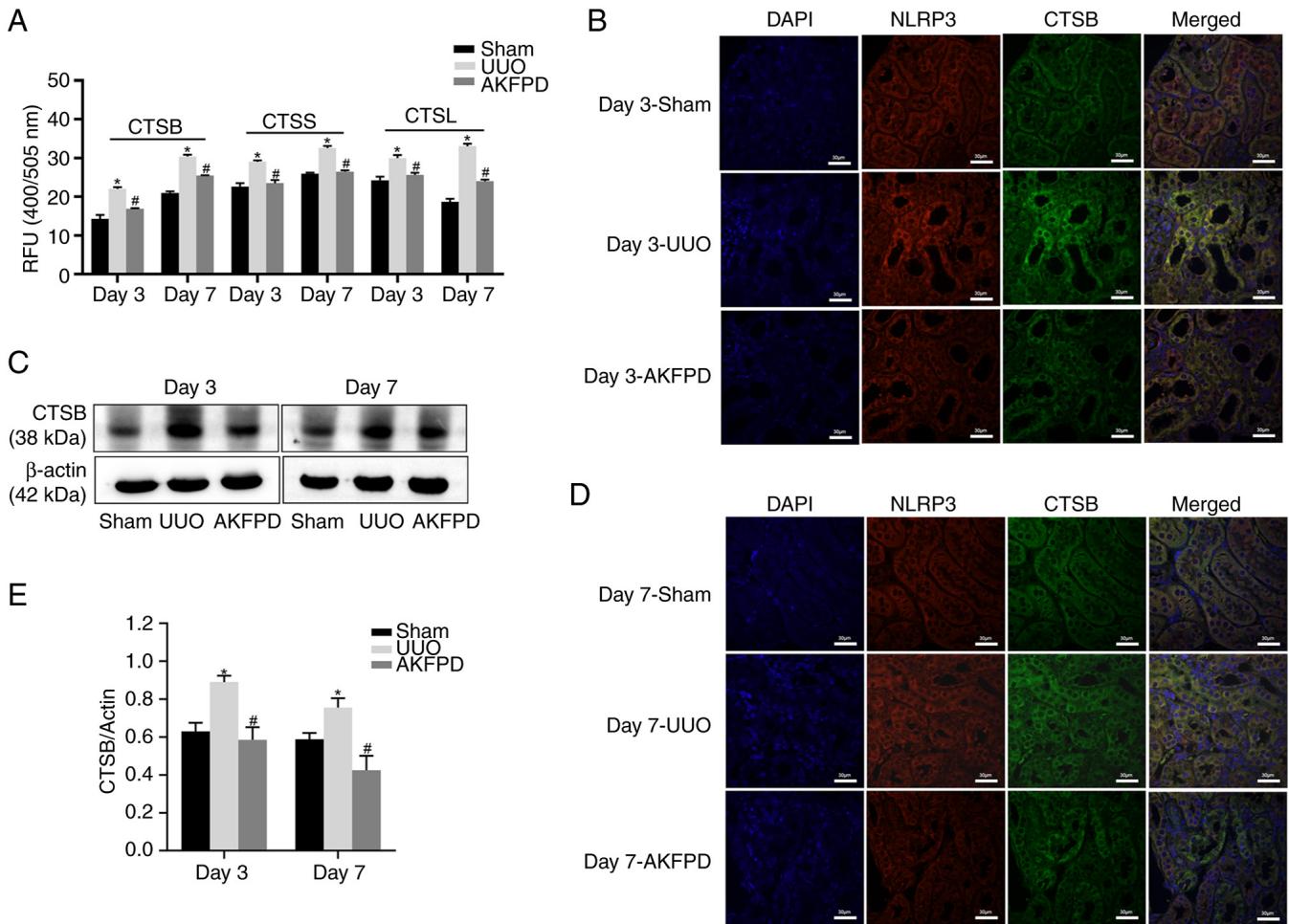


Figure 7. AKFPD inhibits CTSB-mediated NLRP3 inflammasome activation in UUO rats. (A) Effects of AKFPD on cathepsin (CTSB, CTSS and CTSL) activities in the rat kidney tissues. (B) Effects of AKFPD on the colocalization of NLRP3 and CTSB in the rat kidney tissues visualized using immunostaining in UUO rats on day 3 (magnification, x400; scale bar, 30 μm). (C) Representative western blot of CTSB in the rat kidney tissues. (D) Effects of AKFPD on the colocalization of NLRP3 and CTSB in the rat kidney tissues visualized using immunostaining in UUO rats on day 7 (magnification, x400; scale bar, 30 μm). (E) Quantitative data of CTSB in the rat kidney tissues. Data are presented as mean ± standard deviation (n=5 per group). \*P<0.05 vs. sham group, #P<0.05 vs. UUO group. AKFPD, fluorofenidone; CTSB, cathepsin B; NLRP3, NOD-like receptor thermal protein domain associated protein 3; UUO, unilateral ureteral obstruction; CTSS, cathepsin S; CTSL, cathepsin L.

*in vitro* experiment results, treatment with AKFPD down-regulated cathepsin activity *in vivo*. A number of studies have shown that lysosomal damage causes lysosomal membrane destabilization and releases large amounts of CTSB into the cytoplasm, which plays a critical role in NLRP3 inflammasome activation and is required for caspase-1 activation and IL-1β production (54,55). As CTSB plays a critical role in NLRP3 inflammasome activation, the present study focused on the effect of AKFPD on the activation of the NLRP3 inflammasome by CTSB. The findings indicated that AKFPD plays a role in suppressing the expression of CTSB, thereby inhibiting its involvement in NLRP3 inflammasome activation. Therefore, the present study provided novel insights into the mechanism by which AKFPD inhibits NLRP3 inflammasome activation.

In the present study, the abundance of lysosomes increased upon stimulation *in vitro* and was significantly decreased by treatment with AKFPD. As previously reported, the formation of autolysosomes contributes to the elimination of damaged lysosomes (5). Therefore, these results suggested that AKFPD may also enhance the autophagic-lysosomal

degradation pathway to eliminate damaged lysosomes. Furthermore, increasing evidence suggests that autophagy reduces the expression of NLRP3 inflammasome-associated cytokines, thereby suppressing inflammation (56). These findings indicate a new mechanism by which AKFPD inhibits inflammation via the suppression of NLRP3 inflammasome activation.

The present study had some limitations, including the lack of a comprehensive investigation of the underlying mechanisms using knockout or overexpression experiments.

The present study confirmed that AKFPD alleviates renal fibrosis by suppressing lysosomal cathepsin-mediated activation of the NLRP3 inflammasome. However, further studies are required to confirm whether AKFPD affects the autolysosome pathway.

#### Acknowledgements

The authors would like to thank Professor Lijian Tao (Department of Nephrology, Xiangya Hospital of Central South University, Changsha, China) for providing AKFPD.

## Funding

The present study was supported by the National Natural Science Foundation of China (grant no. 81960678) and the Natural Science Foundation of Jiangxi Province (grant no. 20181BAB215010).

## Availability of data and materials

The data generated in the present study may be requested from the corresponding author.

## Authors' contributions

LZhe, YY and XW designed the present study. LZhe, WM, ZH, XL and WL performed the experiments. LZha, JZ, QW and JL analyzed the data. LZhe and YY wrote the manuscript. LZhe and YY confirm the authenticity of all the raw data. All authors have read and approved the final version of the manuscript.

## Ethics approval and consent to participate

The present study protocol was approved by the Medical Research Ethics Committee of the First Affiliated Hospital of Nanchang University (approval no. 2020-1-59).

## Patient consent for publication

Not applicable.

## Competing interests

The authors declare they have no competing interests.

## References

- Hackl MJ, Burford JL, Villanueva K, Lam L, Suszták K, Schermer B, Benzing T and Peti-Peterdi J: Tracking the fate of glomerular epithelial cells in vivo using serial multiphoton imaging in new mouse models with fluorescent lineage tags. *Nat Med* 19: 1661-1666, 2013.
- Lovisa S, LeBleu VS, Tampe B, Sugimoto H, Vадnagara K, Carstens JL, Wu CC, Hagos Y, Burckhardt BC, Pentcheva-Hoang T, *et al*: Epithelial-to-mesenchymal transition induces cell cycle arrest and parenchymal damage in renal fibrosis. *Nat Med* 21: 998-1009, 2015.
- Li X, Pan J, Li H, Li G, Liu X, Liu B, He Z, Peng Z, Zhang H, Li Y, *et al*: DsbA-L mediated renal tubulointerstitial fibrosis in UUO mice. *Nat Commun* 11: 4467, 2020.
- Meng XM, Nikolic-Paterson DJ and Lan HY: Inflammatory processes in renal fibrosis. *Nat Rev Nephrol* 10: 493-503, 2014.
- Kimura T, Isaka Y and Yoshimori T: Autophagy and kidney inflammation. *Autophagy* 13: 997-1003, 2017.
- Jo EK, Kim JK, Shin DM and Sasakawa C: Molecular mechanisms regulating NLRP3 inflammasome activation. *Cell Mol Immunol* 13: 148-159, 2016.
- Alyaseer AAA, de Lima MHS and Braga TT: The role of NLRP3 inflammasome activation in the epithelial to mesenchymal transition process during the fibrosis. *Front Immunol* 11: 883, 2020.
- Song H, Zhao C, Yu Z, Li Q, Yan R, Qin Y, Jia M and Zhao W: UAF1 deubiquitinase complexes facilitate NLRP3 inflammasome activation by promoting NLRP3 expression. *Nat Commun* 11: 6042, 2020.
- Bakker PJ, Butter LM, Claessen N, Teske GJ, Sutterwala FS, Florquin S and Leemans JC: A tissue-specific role for Nlrp3 in tubular epithelial repair after renal ischemia/reperfusion. *Am J Pathol* 184: 2013-2022, 2014.
- Vilaysane A, Chun J, Seamone ME, Wang W, Chin R, Hirota S, Li Y, Clark SA, Tschopp J, Trpkov K, *et al*: The NLRP3 inflammasome promotes renal inflammation and contributes to CKD. *J Am Soc Nephrol* 21: 1732-1744, 2010.
- He H, Jiang H, Chen Y, Ye J, Wang A, Wang C, Liu Q, Liang G, Deng X, Jiang W and Zhou R: Oridonin is a covalent NLRP3 inhibitor with strong anti-inflammasome activity. *Nat Commun* 9: 2550, 2018.
- Kim SM, Kim YG, Kim DJ, Park SH, Jeong KH, Lee YH, Lim SJ, Lee SH and Moon JY: Inflammasome-independent role of NLRP3 mediates mitochondrial regulation in renal injury. *Front Immunol* 9: 2563, 2018.
- Cocchiari P, De Pasquale V, Della Morte R, Tafuri S, Avallone L, Pizard A, Moles A and Pavone LM: The multifaceted role of the lysosomal protease cathepsins in kidney disease. *Front Cell Dev Biol* 5: 114, 2017.
- Fox C, Cocchiari P, Oakley F, Howarth R, Callaghan K, Leslie J, Luli S, Wood KM, Genovese F, Sheerin NS and Moles A: Inhibition of lysosomal protease cathepsin D reduces renal fibrosis in murine chronic kidney disease. *Sci Rep* 6: 20101, 2016.
- Musante L, Tataruch D, Gu D, Liu X, Forsblom C, Groop PH and Holthofer H: Proteases and protease inhibitors of urinary extracellular vesicles in diabetic nephropathy. *J Diabetes Res* 2015: 289734, 2015.
- Tang TT, Lv LL, Pan MM, Wen Y, Wang B, Li ZL, Wu M, Wang FM, Crowley SD and Liu BC: Hydroxychloroquine attenuates renal ischemia/reperfusion injury by inhibiting cathepsin mediated NLRP3 inflammasome activation. *Cell Death Dis* 9: 351, 2018.
- Allan ERO, Campden RI, Ewanchuk BW, Tailor P, Balce DR, McKenna NT, Greene CJ, Warren AL, Reinheckel T and Yates RM: A role for cathepsin Z in neuroinflammation provides mechanistic support for an epigenetic risk factor in multiple sclerosis. *J Neuroinflammation* 14: 103, 2017.
- Meng J, Zou Y, Hu C, Zhu Y, Peng Z, Hu G, Wang Z and Tao L: Fluorofenidone attenuates bleomycin-induced pulmonary inflammation and fibrosis in mice via restoring caveolin 1 expression and inhibiting mitogen-activated protein kinase signaling pathway. *Shock* 38: 567-573, 2012.
- Peng ZZ, Hu GY, Shen H, Wang L, Ning WB, Xie YY, Wang NS, Li BX, Tang YT and Tao LJ: Fluorofenidone attenuates collagen I and transforming growth factor-beta1 expression through a nicotinamide adenine dinucleotide phosphate oxidase-dependent way in NRK-52E cells. *Nephrology (Carlton)* 14: 565-572, 2009.
- Peng Y, Yang H, Zhu T, Zhao M, Deng Y, Liu B, Shen H, Hu G, Wang Z and Tao L: The antihepatic fibrotic effects of fluorofenidone via MAPK signalling pathways. *Eur J Clin Invest* 43: 358-368, 2013.
- Ning WB, Hu GY, Peng ZZ, Wang L, Wang W, Chen JY, Zheng X, Li J and Tao LJ: Fluorofenidone inhibits Ang II-induced apoptosis of renal tubular cells through blockage of the Fas/FasL pathway. *Int Immunopharmacol* 11: 1327-1332, 2011.
- Tu S, Jiang Y, Cheng H, Yuan X, He Y, Peng Y, Peng X, Peng Z, Tao L and Yang H: Fluorofenidone protects liver against inflammation and fibrosis by blocking the activation of NF- $\kappa$ B pathway. *FASEB J* 35: e21497, 2021.
- Tang Y, Zhang F, Huang L, Yuan Q, Qin J, Li B, Wang N, Xie Y, Wang L, Wang W, *et al*: The protective mechanism of fluorofenidone in renal interstitial inflammation and fibrosis. *Am J Med Sci* 350: 195-203, 2015.
- Kocak MZ, Aktas G, Atak BM, Duman TT, Yis OM, Erkuş E and Savlı H: Is Neuregulin-4 a predictive marker of microvascular complications in type 2 diabetes mellitus? *Eur J Clin Invest* 50: e13206, 2020.
- Bilgin S, Kurtkulagi O, Atak Tel BM, Duman TT, Kahveci G, Khalid A and Aktas G: Does C-reactive protein to serum albumin ratio correlate with diabetic nephropathy in patients with type 2 diabetes mellitus? The care time study. *Prim Care Diabetes* 15: 1071-1074, 2021.
- Aktas G, Yilmaz S, Kantarci DB, Duman TT, Bilgin S, Balci SB and Atak Tel BM: Is serum uric acid-to-HDL cholesterol ratio elevation associated with diabetic kidney injury? *Postgrad Med* 135: 519-523, 2023.
- Taslamacioglu Duman T, Ozkul FN and Balci B: Could systemic inflammatory index predict diabetic kidney injury in type 2 diabetes mellitus? *Diagnostics (Basel)* 13: 2063, 2023.
- Zheng L, Zhang J, Yuan X, Tang J, Qiu S, Peng Z, Yuan Q, Xie Y, Mei W, Tang Y, *et al*: Fluorofenidone attenuates interleukin-1 $\beta$  production by interacting with NLRP3 inflammasome in unilateral ureteral obstruction. *Nephrology (Carlton)* 23: 573-584, 2018.

29. Liao X, Jiang Y, Dai Q, Yu Y, Zhang Y, Hu G, Meng J, Xie Y, Peng Z and Tao L: Fluorofenidone attenuates renal fibrosis by inhibiting the mtROS-NLRP3 pathway in a murine model of folic acid nephropathy. *Biochem Biophys Res Commun* 534: 694-701, 2021.
30. Chevalier RL, Forbes MS and Thornhill BA: Ureteral obstruction as a model of renal interstitial fibrosis and obstructive nephropathy. *Kidney Int* 75: 1145-1152, 2009.
31. Lu M, Li H, Liu W, Zhang X, Li L and Zhou H: Curcumin attenuates renal interstitial fibrosis by regulating autophagy and retaining mitochondrial function in unilateral ureteral obstruction rats. *Basic Clin Pharmacol Toxicol* 128: 594-604, 2021.
32. Lu M, Yang W, Peng Z, Zhang J, Mei W, Liu C, Tang J, Ma H, Yuan X, Meng J, *et al*: Fluorofenidone inhibits macrophage IL-1 $\beta$  production by suppressing inflammasome activity. *Int Immunopharmacol* 27: 148-153, 2015.
33. Zhang J, Zheng L, Yuan X, Liu C, Yuan Q, Xie F, Qiu S, Peng Z, Tang Y, Meng J, *et al*: Mefenidone ameliorates renal inflammation and tubulointerstitial fibrosis via suppression of IKK $\beta$  phosphorylation. *Int J Biochem Cell Biol* 80: 109-118, 2016.
34. Xiang H, Zhu F, Xu Z and Xiong J: Role of inflammasomes in kidney diseases via both canonical and non-canonical pathways. *Front Cell Dev Biol* 8: 106, 2020.
35. Imig JD and Ryan MJ: Immune and inflammatory role in renal disease. *Compr Physiol* 3: 957-976, 2013.
36. Jiang Y, Quan J, Chen Y, Liao X, Dai Q, Lu R, Yu Y, Hu G, Li Q, Meng J, *et al*: Fluorofenidone protects against acute kidney injury. *FASEB J* 33: 14325-14336, 2019.
37. Seo JB, Choi YK, Woo HI, Jung YA, Lee S, Lee S, Park M, Lee IK, Jung GS and Park KG: Gemigliptin attenuates renal fibrosis through down-regulation of the NLRP3 inflammasome. *Diabetes Metab J* 43: 830-839, 2019.
38. Zheng Z, Xu K, Li C, Qi C, Fang Y, Zhu N, Bao J, Zhao Z, Yu Q, Wu H and Liu J: NLRP3 associated with chronic kidney disease progression after ischemia/reperfusion-induced acute kidney injury. *Cell Death Discov* 7: 324, 2021.
39. Bhatia D, Chung KP, Nakahira K, Patino E, Rice MC, Torres LK, Muthukumar T, Choi AM, Akchurin OM and Choi ME: Mitophagy-dependent macrophage reprogramming protects against kidney fibrosis. *JCI Insight* 4: e132826, 2019.
40. Lorenz G, Darisipudi MN and Anders HJ: Canonical and non-canonical effects of the NLRP3 inflammasome in kidney inflammation and fibrosis. *Nephrol Dial Transplant* 29: 41-48, 2014.
41. Conley SM, Abais JM, Boini KM and Li PL: Inflammasome activation in chronic glomerular diseases. *Curr Drug Targets* 18: 1019-1029, 2017.
42. Orłowski GM, Colbert JD, Sharma S, Bogyo M, Robertson SA and Rock KL: Multiple cathepsins promote Pro-IL-1 $\beta$  synthesis and NLRP3-Mediated IL-1 $\beta$  activation. *J Immunol* 195: 1685-1697, 2015.
43. Kelley N, Jeltama D, Duan Y and He Y: The NLRP3 inflammasome: An overview of mechanisms of activation and regulation. *Int J Mol Sci* 20: 3328, 2019.
44. Martine P and Rébé C: Heat shock proteins and inflammasomes. *Int J Mol Sci* 20: 4508, 2019.
45. Bozic M, Caus M, Rodrigues-Diez RR, Pedraza N, Ruiz-Ortega M, Garí E, Galle P, Panadés MJ, Martínez A, Fernández E and Valdivielso JM: Protective role of renal proximal tubular alpha-synuclein in the pathogenesis of kidney fibrosis. *Nat Commun* 11: 1943, 2020.
46. Dai Q, Zhang Y, Liao X, Jiang Y, Lv X, Yuan X, Meng J, Xie Y, Peng Z, Yuan Q, *et al*: Fluorofenidone alleviates renal fibrosis by inhibiting necroptosis through RIPK3/MLKL pathway. *Front Pharmacol* 11: 534775, 2020.
47. Yang H, Zhang W, Xie T, Wang X and Ning W: Fluorofenidone inhibits apoptosis of renal tubular epithelial cells in rats with renal interstitial fibrosis. *Braz J Med Biol Res* 52: e8772, 2019.
48. Wu M, Han W, Song S, Du Y, Liu C, Chen N, Wu H, Shi Y and Duan H: NLRP3 deficiency ameliorates renal inflammation and fibrosis in diabetic mice. *Mol Cell Endocrinol* 478: 115-125, 2018.
49. Mulay SR: Multifactorial functions of the inflammasome component NLRP3 in pathogenesis of chronic kidney diseases. *Kidney Int* 96: 58-66, 2019.
50. Li L, Tang W and Yi F: Role of inflammasome in chronic kidney disease. *Adv Exp Med Biol* 1165: 407-421, 2019.
51. Lamkanfi M: Emerging inflammasome effector mechanisms. *Nat Rev Immunol* 11: 213-220, 2011.
52. Man SM and Kanneganti TD: Regulation of inflammasome activation. *Immunol Rev* 265: 6-21, 2015.
53. Terada K, Yamada J, Hayashi Y, Wu Z, Uchiyama Y, Peters C and Nakanishi H: Involvement of cathepsin B in the processing and secretion of interleukin-1 $\beta$  in chromogranin A-stimulated microglia. *Glia* 58: 114-124, 2010.
54. Stancu IC, Cremers N, Vanrusselt H, Couturier J, Vanoosthuysse A, Kessels S, Lodder C, Brône B, Huaux F, Octave JN, *et al*: Aggregated Tau activates NLRP3-ASC inflammasome exacerbating exogenously seeded and non-exogenously seeded Tau pathology in vivo. *Acta Neuropathol* 137: 599-617, 2019.
55. Chevriaux A, Pilot T, Derangere V, Simonin H, Martine P, Chalmin F, Ghiringhelli F and Rébé C: Cathepsin B is required for NLRP3 inflammasome activation in macrophages, through NLRP3 interaction. *Front Cell Dev Biol* 8: 167, 2020.
56. Nakahira K, Haspel JA, Rathinam VA, Lee SJ, Dolinay T, Lam HC, Englert JA, Rabinovitch M, Cernadas M, Kim HP, *et al*: Autophagy proteins regulate innate immune responses by inhibiting the release of mitochondrial DNA mediated by the NALP3 inflammasome. *Nat Immunol* 12: 222-230, 2011.



Copyright © 2024 Zheng et al. This work is licensed under a Creative Commons Attribution-NonCommercial-NoDerivatives 4.0 International (CC BY-NC-ND 4.0) License.